

# LIFETIME STUDY OF TUNGSTEN FILAMENTS IN AN H<sup>-</sup> SURFACE CONVERTER ION SOURCE\*

I.N. Draganic<sup>#</sup>, J. F. O'Hara, and L. Rybarcyk, LANL, Los Alamos, NM 87545, USA

## Abstract

The tungsten filaments are critical components that limit the lifetime of the H<sup>-</sup> surface converter ion source. Their finite lifetime has a huge impact on the maintenance schedules and overall availability of an accelerator facility. We present in this work a simple analytical filament lifetime model and 3D thermal simulation explaining basic phenomena of filament erosion and electrical resistance changes during a normal run of an H<sup>-</sup> production ion source at the Los Alamos Neutron Science Center (LANSCC). The calculation of filament longitudinal temperature profile takes into consideration the effects of ohmic heating, thermal conductivity and total emissivity for tungsten wires in high vacuum. The simulation includes the DC voltage operation of the filament with and without pulsed arc discharge current and gives the differential filament resistance changes, metal evaporation rates and theoretical electron emission currents. The results of the computation are compared with observed experimental data recorded using the EPICS control system during a normal LANSCC production cycle of 28 days with pulse repetition of 60 Hz and duty factor of 5%.

## H<sup>-</sup> ION SOURCE LIFETIME

H<sup>-</sup> surface converter ion sources are well described elsewhere [1-4]. Three nearly-identical H<sup>-</sup> radial extraction converter ion sources (see Fig. 1A) have been utilized for proton beam production at LANSCC for more than 25 years. These H<sup>-</sup> sources deliver typical beam current up to 18 mA into an 80-kV electrostatic column and have operational lifetimes more than four weeks between accelerators maintains periods at a repetition rate of 60 Hz and duty factor of 5%. Typical EPICS-recorded data of the extracted H<sup>-</sup> ion beams and an evolution of each filament's relative differential resistance during an entire cycle are presented in Figure 2. The negative-ion source consists of a filament driven arc discharge in a permanent-magnet, multi-cusp vacuum chamber for plasma confinement and a negatively biased converter electrode for H<sup>-</sup> beam production. The source uses two filaments made of high purity tungsten wires (99.99%), bent in a characteristic shape (see Figure 1B) with length of 297 mm, 1.6 mm thick diameter, weight of ~12 g and resistance of 7.8 mΩ at 295 K. Nominal filament currents of 100 to 106 A are driven by DC constant voltage power supplies (11 - 12V) bringing the wires to working temperature range of 2600 to 2700 K. The increase of filament temperature for higher electron output (plasma discharge) or more intense H<sup>-</sup> current is limited by the increasing of evaporation of filament material, which

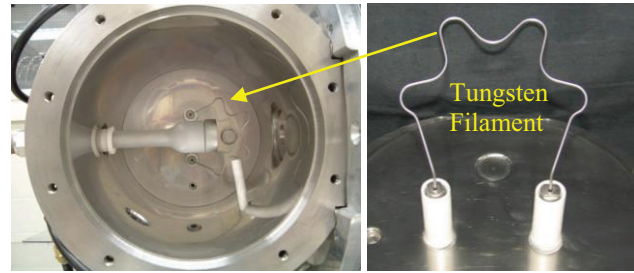


Figure 1: An internal side view of the LANSCC H<sup>-</sup> ion source is shown (A). New tungsten wire mounted on the water cooled ports (B).

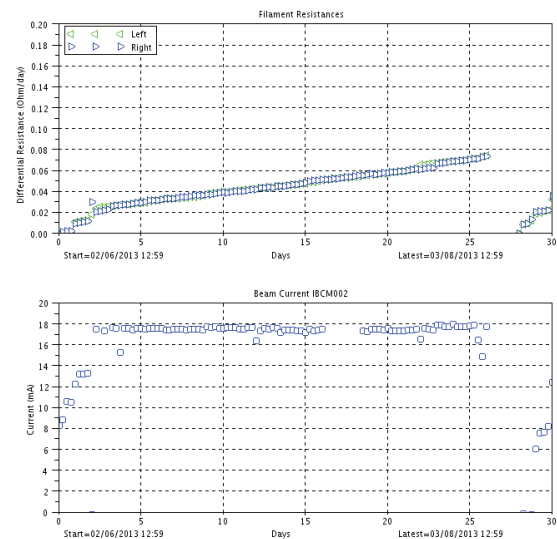


Figure 2: An EPICS application plots for operation monitoring purposes the filament relative differential resistances and the 80 keV extracted beam currents during a LANSCC beam production cycle (points every 6 hours).

decreases the lifetimes of the filaments, and ultimately limits the ion source operating period before replacement. The characteristics of tungsten filaments in vacuum at various high temperatures were studied in detail for incandescent lamps, radio tubes and in other scientific and engineering investigations [5-12]. There are two empirical criteria for critical differential resistance that predict the onset of filament failure: a) 12% of total increase in filament resistance or decrease in mass weight [5, 6] and b) 19 % of total increase in filament resistance or 10% of reduction in wire diameter [4, 8-12].

## FILAMENT RELATIVE DIFFERENTIAL RESISTANCE

The LANSCC EPICS control system continuously records (a sample per minute) the filament currents and voltages, as well as the arc discharge peak currents and voltages. The filament resistances, based on U/I

\*Work supported by the US Department of Energy under Contract Number DE-AC52-06NA25396

<sup>#</sup>draganic@lanl.gov

measurements, change in the range from 100 to 115 m $\Omega$  (Figure 3A). The hot wire resistance increases over 140 times from the room temperature resistance. Differential resistance is calculated using a simple formula:

$$\frac{\Delta R}{R} = \frac{R_2 - R_1}{R_1} = \frac{R_2}{R_1} - 1 = \frac{U_2 I_1}{U_1 I_2} - 1 \quad (1)$$

where  $R_1$  is the filament resistance at beginning of run ( $t_1=0$ ) and  $R_2$  is resistance recorded later during the cycle ( $t_2 \neq t_1$ ). A characteristic relative differential resistance increase of 7.5% is shown in Figure 3B staying well below the 12% criteria. Digitized resistance data (40,000 points over 28 days) obtained using EPICS, enables easy data access and manipulation. The new filaments were weighed prior to installation and refurbishment to determine their mass, and later, after the production cycle and filament disassembly. The mass measurements are presented in Table 1. An average tungsten evaporation rate of 27 mg/day was observed. Measured relative mass changes were 2% less than the recorded differential resistances. Even after a correction for the inserted wire length into holder/ports, the discrepancy between mass and relative resistance measurements was considerable. Step-wise changes in both differential resistance graphs were observed during adjusting of the DC heating currents and source optimization. Systematic errors in differential resistances due to the long connection cables, shunts and voltage readings are being neglected.

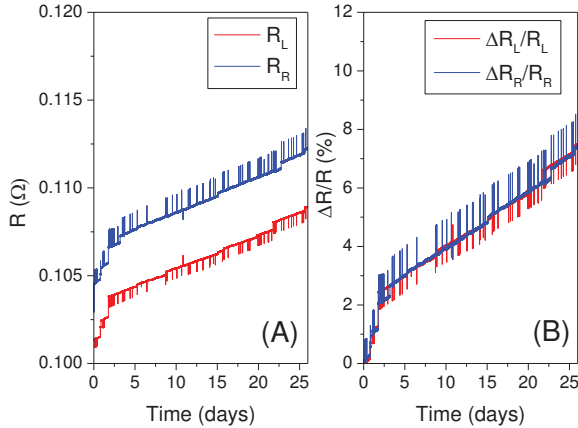


Figure 3: Characteristic filament resistances and relative differential resistances calculated using EPICS recorded U/I measurement data for both filaments.

Table 1: Mass Measurements and Recorded Differential Resistances from the EPICS Data are Listed.  $\Delta M/M^*$  is a Length Corrected Evaporated Mass ( $k=1.072$ ).

Filament	Left (#1)	Right (#1)
M1 (g) (before)	11.808	11.737
M1 (g) (after)	11.134	11.020
$\Delta M$ (g)	0.674	0.717
$\Delta M/M$ (%)	5.71	6.12
$\Delta M/M^*$ (%)	6.12	6.56
$\Delta R/R$ (%)	7.5	7.44

## FILAMENT RESISTANCE MODEL

A simple analytical filament resistance model is needed to explain the wire erosion and recorded differential resistance behavior. The model has the following assumptions: a) an ideal wire is considered; it has a constant position/shape (no plastic deformation, sagging etc.), b) the filament temperature is constant across the wire length, c) thermal expansion is negligible, d) the mass evaporation is uniform over the wire surface and is a function of temperature, e) the total emissivity for tungsten wire varies only with temperature, f) the filament current is a sum of DC heating current and peak arc discharge current averaged by the duty factor, g) plasma sputtering is not taken into account, and h) microscopic effects like a recrystallization, grain growth, impurity content, electro-migration (Soret's effect) are not included [12]. The tungsten wire resistance is described using dimensional formula  $R_i = \rho_i L_i / S_i$ , for  $i=1$  ( $t_1=0$ ),  $i=2$  ( $t_2 \neq t_1$ );  $L$  and  $S$  are the wire length and cross section respectively. Because the filaments have very small thermal expansion differences ( $L_1 \approx L_2$ ), equation (1) can be simplified:

$$\frac{\Delta R}{R} = \frac{\rho_1 S_2 L_1}{\rho_2 S_1 L_2} - 1 \approx \frac{\rho_1 S_2}{\rho_2 S_1} - 1 \quad (2)$$

In our model, the specific electrical resistance is a linear function of temperature ( $\rho_i = a + bT_i$ ). The time averaged mass evaporation is defined by the equation  $\Gamma = \Delta M / A_c \Delta t$  or  $\Gamma = (\rho_m L \Delta S) / (A_c \Delta t)$ , where  $\Gamma$  (g/cm<sup>3</sup>/s) is an evaporation rate [6, 11],  $A_c$  is the wire evaporation surface area,  $\Delta M$  and  $\Delta t$  are evaporated mass and evaporation time,  $\Delta S$  is a reduction in wire cross section and  $\rho_m$  is tungsten mass density (19.25 g/cm<sup>3</sup>) [13]. Equation (2) can then be rewritten in the form:

$$\frac{\Delta R}{R} = \frac{b(T_2 - T_1)}{\rho_1} + \frac{\Gamma(T_1) A_c \Delta t}{S_1 \rho_m L} = \frac{b \Delta T}{\rho_1} + \frac{\Delta M}{M_1} \quad (3)$$

Equation (3) has two components. The first term takes into account material electrical characteristics and changes in filament temperature with filament current. This term represents “fast” processes and is independent of time, describes the tuning processes. The second term describes the “slow” processes including filament evaporation and steady state changes in filament mass and cross section. This time dependent term is a useful monitoring tool for the filament and source lifetime.

The filament temperature in our model is determined from the graphs presented in Ref. [6]. The temperature is defined by the heating current through filament,  $I$ , and the wire diameter  $d$ . For our model, we have created a two dimension polynomial fit to the data [6]: (surface function  $T(K) = A_0 + A_1 d + A_2 I + A_3 d^2 + A_4 I^2 + A_5 I d$ ).

The filament resistance model was applied to simulate the experimentally recorded data in Figure 2. Using estimated wire diameter after processing of H-source and recording total current for the left filament, calculation of the temperature was possible. Results of mass losses integrated over the run cycle and  $\Delta R/R$  step changes are presented in Figure 4 and Table 2 showing a reasonable agreement with recorded data.

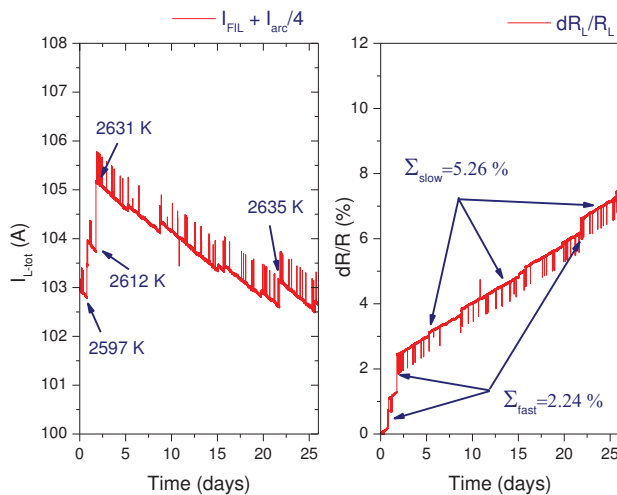


Figure 4: (A) Measured total left-filament current as a function of days during the run cycle. Also shown are associated changes in wire temperature after each source adjustment. (B) Measured left-filament differential resistance. Percent changes in differential resistances due “fast” and “slow” processes are shown.

Table 2: Measured Left Filament Differential Resistance Compared with Filament Model Calculation

Filament	Total (%)	Fast (%)	Slow (%)
EPICS data	7.50	2.24	5.26
Model	7.11	1.76	5.35

## THERMAL FINITE ELEMENT ANALYSIS

A thermal finite element analysis was also performed to determine a steady state temperature profile. A 3D model of the tungsten filament was created. Included in the filament thermal simulations are the tungsten physical properties, ohmic heating, thermal conductivity and thermal emissivity in high vacuum [13]. A constant heating current of 103.5 A is applied to the filament. Arc current ranging from 0.75 A to zero is assumed to be decreasing linearly from one end of the filament to the other (discretized in 10 steps). Radiation and temperature boundary conditions across all wire segments are applied for 294 K at each end (due to water cooling loops). The total emissivity varies as a function of wire segment temperature. A peak filament temperature of 2684 K was calculated. The peak temperature moves from the center of the filament towards the higher-arc-current side (Fig. 5A). As the filament evaporates in a localized area close to the peak temperature location, the cross section of the filament decreases in that area. This decrease in cross sectional area causes an increase in resistance, which results in an even higher temperature for the same applied currents. This creates a runaway situation of decreasing wire cross section, increasing temperature and high evaporation rate that leads to creation of a localized hot spot that can cause catastrophic failure of the filament [7]. This typical filament failure mode is shown in Figure 5B.

We propose changing the polarity of the DC filament and arc voltages at least once per week in order to avoid hot spots created by this asymmetric ohmic heating.

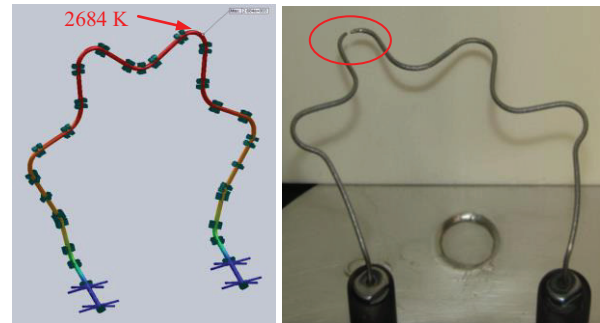


Figure 5: (A) 3D model of source filament and calculated temperature profile with the maximum-temperature location shown. (B) Photo showing a filament with a typical hot spot - breaking point failure.

## ACKNOWLEDGEMENT

The authors are thankful to Jerry Paul and Nathan Okamoto for the filament mass measurements, production source processing stand data and source photos.

## REFERENCES

- [1] Bernhard Wolf, “Handbook of Ion Sources” (1995).
- [2] Ian G. Brown, “The Physics and Technology of Ion Source” (2004).
- [3] J. Sherman, et al. ” Physical Insights and Test Stand Results for the LANSCE H Surface Converter Source”, AIP Conf. Proc. **763**, AIP, Melville, NY, p.254 (2005).
- [4] R. Keller, et al. “H<sup>-</sup> Ion Source Development for the LANSCE Accelerator Systems”, AIP Con.Proc. **1097**, AIP, Melville, NY, p. 161 (2009).
- [5] G. Rouleau et al. “Tungsten Filament material and Cs dynamic equilibrium effects on a surface converter ion source” Rev. Sci. Instrum. **79**, 02A514 (2008).
- [6] M. Ardenne “Tabellen zur Angewandten Physik” (1963, Berlin) Band I and II.
- [7] E. Chacon- Golcher, “Erosion and Failure of Tungsten Filament”, LA-UR-08-5251 (2008).
- [8] J. Röhrlich, et.al. “A Tandetron as proton injector for the eye tumor therapy in Berlin” Rev. Sci. Instrum. **83**, 02B903 (2012).
- [9] A. Wilson, “Tungsten filament lifetime under constant-current heating”, J. App. Phys, **40**, 1956, (1969).
- [10] R. N. Bloomer, “High temperature properties of tungsten which influence filament temperatures, lives and thermionic-emission densities” Proc. IEEE, **B104**, 157, (1957).
- [11] H.A. Jones and I. Langmuir, “The characteristics of Tungsten Filaments as Function of Temperature” General Electric Review, **30**, part I p 310, part II p 354, part III p408, (1927).
- [12] R.P. Johnson, “Construction of Filament Surfaces”, Phys. Rev., **54**, (1938) p459.
- [13] “American Society of Materials - Metals Handbook” Edit by R. L. Stedfeld (1990) Vol. 2.